UCL CENTRE FOR ADVANCED SPATIAL ANALYSIS

UCL

WORKING PAPERS SERIES

Paper 171 - Nov 11

Introducing space to mathematical models of conflict

ISSN 1467-1298

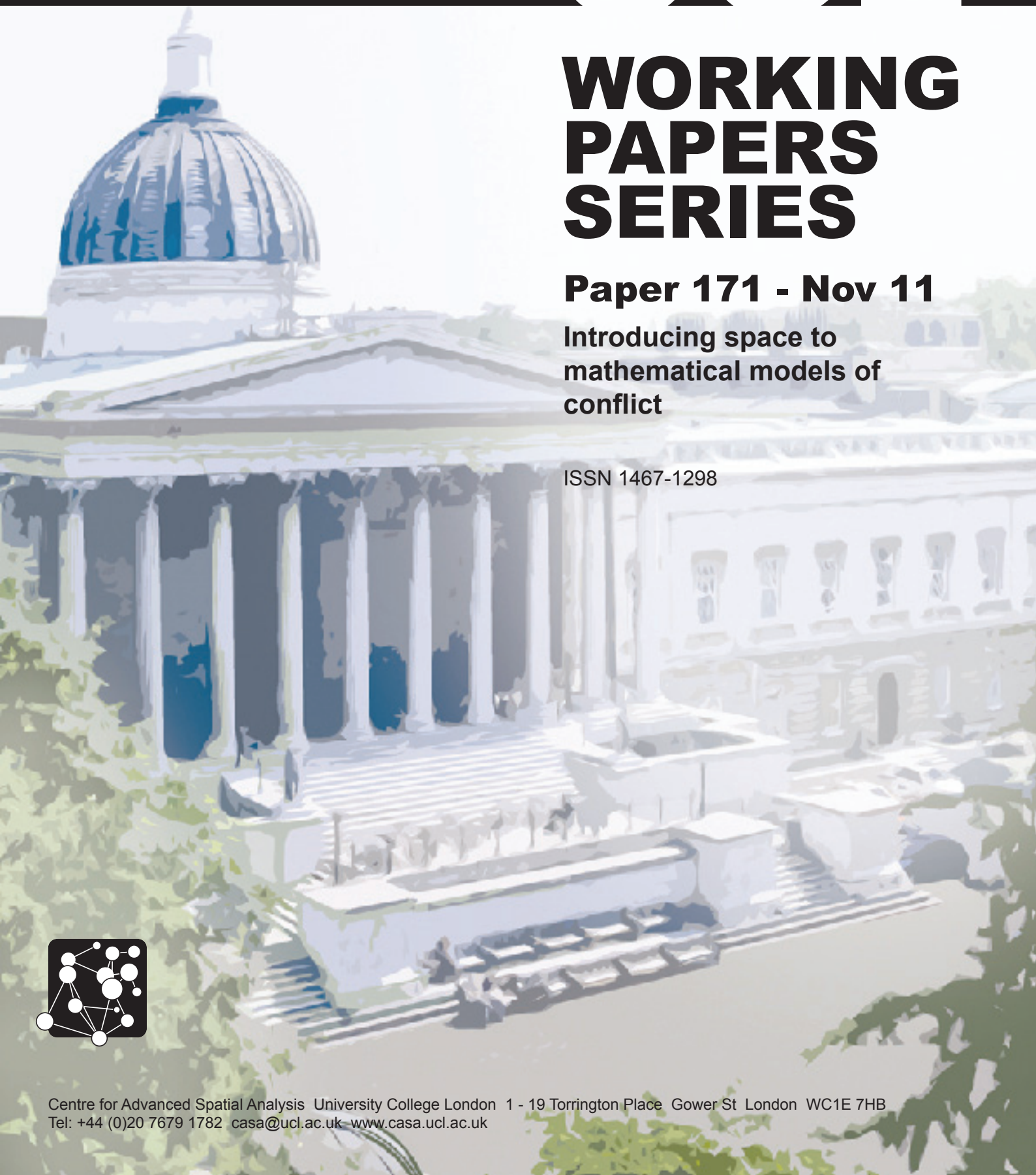

Centre for Advanced Spatial Analysis University College London 1 - 19 Torrington Place Gower St London WC1E 7HB
Tel: +44 (0)20 7679 1782 casa@ucl.ac.uk www.casa.ucl.ac.uk

Introducing space to mathematical models of conflict.*

P. Baudains, H.M. Fry, T.P. Davies, A.G. Wilson

November 1, 2011

1 Introduction

Dynamic ecological models of interacting populations have been used extensively to investigate conflict between adversaries. Common examples include the Lotka-Volterra equations for predator-prey relationships, Lanchester equations for direct combat and Richardson equations for arms races and conflict escalation. Modelling the evolution of conflict is of value to military strategists as well as to policy-makers: the former may develop very detailed models which include extensive considerations of terrain, available resources and specific short-term objectives, while the latter may be interested in identifying mechanisms that may lead to conflict, strategies for achieving long-term objectives, or highlighting areas or people that may be at risk of impending conflict.

The existing models of Lotka-Volterra, Lanchester and Richardson share similarities in their underlying dynamics, and may be written in a general form by way of the coupled equations:

$$\begin{aligned} \dot{x} &= (a_1 x + b_1 y + c_1) f(x) \\ \dot{y} &= (a_2 y + b_2 x + c_2) g(y), \end{aligned} \tag{1}$$

where x and y are sizes of two adversaries; a, b, c and d are constants and f and g are given functions. If $f(x) = x$ and $g(y) = y$ then equations (1) are the Lotka-Volterra equations when $a_1 = a_2 = 0$, $b_1, c_2 < 0$ and $b_2, c_1 > 0$ and a version of the Lanchester equations when $a_1 = c_1 = a_2 = c_2 = 0$. If $f(x) = g(x) = 1$ then equations (1) are the Richardson equations when $a_1, a_2 < 0$ and $b_1, b_2 > 0$ and a version of the Lanchester equations when $a_1 = c_1 = a_2 = c_2 = 0$.

*The authors acknowledge the financial support of the Engineering and Physical Sciences Research Council (EPSRC) under the grant ENFOLD-ing - Explaining, Modelling, and Forecasting Global Dynamics, reference EP/H02185X/1.

In many instances of conflict, the spatial distribution of resources (for example, troops or arms) has a significant effect upon both the actions of adversaries and the eventual outcome of the conflict. The possession of territory is often seen as a vital strategic concern during conflict, and may even be the motivation for the conflict itself. Although Figures 1(a) and 1(b) depict scenarios which would be considered as equivalent by the aggregate models, since the overall resources of teams are equal in each, a realistic interpretation would not regard them as such. In Figure 1(a), the blue team's position could be regarded as superior, due to its numerical advantage and the fact that it has 'cornered' red, whereas in 1(b) the blue team is at a disadvantage, having been surrounded by red and having had its force divided by a physical obstacle.

As Epstein (1997) explains, neglecting space in the Lanchester equations of warfare leads to the Lanchester square law which states that stalemate between two adversaries, R and B, occurs when the initial number of resources R_0 and B_0 balance as

$$B_0 = \sqrt{\frac{r}{b}} R_0, \tag{2}$$

where r and b are the effectiveness of the red team and the blue team respectively. Thus, to defeat an opponent who is three times as numerous, it does not suffice to be three times as effective, but rather a team must be nine times as effective. By neglecting space, it is implicitly assumed that total resource levels are the only factors which govern the system, but it may be that, in fact, the distribution of resources has a material effect on real-life outcomes.

It is therefore natural to spatially disaggregate the model in (1), in order to take into account the distribution of resources when evaluating interactions between adversaries. To this end, we derive a measure of 'threat' that is used to model the intimidatory effect of arms located in one position on a team located elsewhere; this is done in section 2. In section 3 we present an example using the Richardson model for conflict escalation, and show the effect of considering space in this way. In section 4 we present some analysis of this model, highlighting the effect of the model parameters. In section 5 we present an example which indicates how spatially disaggregated models of conflict might be used in real-world situations and in section 6 we discuss applicability of this model.

2 Threat as a spatial interaction model

We derive a measure of threat using an entropy maximising spatial interaction model. These models have previously been used to study flows of physical objects (*e.g.* goods, people, money) and a general approach is outlined in Wilson (2008).

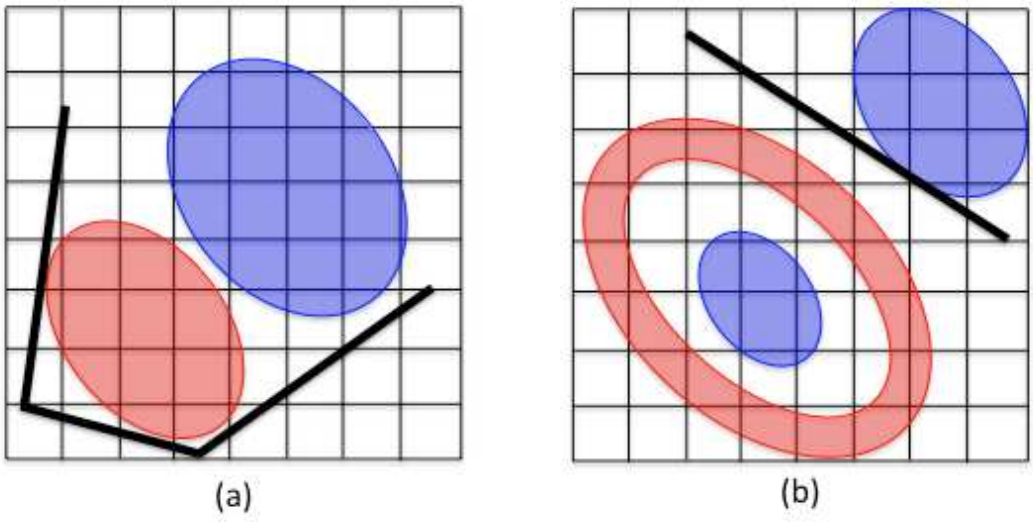

Figure 1: Two examples of red and blue adversaries with different spatial distribution and impedance within the environment to demonstrate the value of incorporating space into models of conflict.

Firstly, we define a discrete zone structure on the spatial area of interest (*i.e.* the area on which interactions between adversaries take place) and label each zone from 1 to N. Let d_{ij} be some measure of distance, cost or impedance between zones i and j for this given zone structure. The measure of threat will be based on the spatial distribution of some resource, for example, the number of arms or troops. Therefore let x_i be the number of resources of x in zone i and y_i the number of resources of y in zone i.

If the amount of threat on y in zone j that is due to the presence of x_i resources of x in zone i is given by T_{ij}^{xy}, then the total amount of threat on y across all zones that can come from resources x_i in i is proportional to the amount of resources in x_i. Thus,

$$\sum_j T_{ij}^{xy} = h_x x_i, \tag{3}$$

where h_x can be thought of as the effectiveness of x in delivering threat or, in other words, an 'intimidation factor' of team x.

Following Wilson (2008), we assume that there is some total 'energy' in this system of imposed threat that must be conserved, so that

$$\sum_{i,j} T_{ij}^{xy} d_{ij} = C_{xy}, \tag{4}$$

for some constant C_{xy}.

We also add the constraint

$$\sum_{i,j} T_{ij}^{xy} \log y_j = B, \tag{5}$$

where $\log y_j$ can be thought of as some 'benefit' derived by team x through exerting threat on y in zone j. Equation (5) constrains the total amount of threat that team x can exert on y.

An estimate of T_{ij}^{xy} is then found by maximising the entropy measure:

$$S = -\sum_{ij} T_{ij}^{xy} \log T_{ij}^{xy}, \tag{6}$$

subject to the constraints (3), (4) and (5). It can be shown that this gives

$$T_{ij}^{xy} = A_i x_i y_j^{\alpha} \exp(-\beta d_{ij}), \tag{7}$$

where

$$A_i = \frac{h_x}{\sum_j y_j^{\alpha} \exp(-\beta d_{ij})}, \tag{8}$$

for parameters α and β. In this simple model we set $\alpha = 1$. This gives us the flow equation:

$$T_{ij}^{xy} = \frac{h_x x_i y_j \exp(-\beta d_{ij})}{\sum_k y_k \exp(-\beta d_{ik})}. \tag{9}$$

The total threat on y in zone j is then

$$\tau_j^y = \sum_i T_{ij}^{xy} \tag{10}$$

$$= \sum_i \frac{h_x x_i y_j \exp(-\beta d_{ij})}{\sum_k y_k \exp(-\beta d_{ik})}, \tag{11}$$

and, since j is arbitrary, this holds for $j = 1, 2, 3, ..., N$. The real-world interpretation of this flow is that threat moves from x in zone i to y in zone j, proportional to the number of resources that x has in zone i, multiplied by the relative weighting of the resources of y in zone j compared with the rest of y's resource in all of the other zones.

Similarly, team y will also exert some threat on team x so, by an analogous derivation, we have that the total threat on x in zone j is given by

$$\tau_j^x = \sum_i T_{ij}^{yx} \tag{12}$$

$$= \sum_i \frac{h_y y_i x_j \exp(-\beta d_{ij})}{\sum_k x_k \exp(-\beta d_{ik})}, \tag{13}$$

Now we have a measure of the total threat on an adversary within a given zone, we can spatially disaggregate a variant of the model in (1). The concept of embedding a spatial interaction model into a wider dynamic algorithm is not novel; Wilson (2008) embeds the Boltzmann technique shown here into Lotka-Volterra dynamics to model the structural change of a retail system.

3 A spatial model of conflict escalation

As an example, we use our measure of spatially-varying threat to disaggregate the Richardson model of conflict escalation. We are interested in how threat, conceptualised in this way, leads to escalation of conflict over space. We will extend the Richardson version of the equations given in (1):

$$\begin{aligned} \dot{x} &= b_1 y - a_1 x + c_1 \\ \dot{y} &= b_2 x - a_2 y + c_2, \end{aligned} \tag{14}$$

where constants $b_1, a_1, b_2, a_2 \geq 0$. These equations were originally proposed to model the evolution of an arms race. The $b_1 y$ and $b_2 x$ terms are the action-reaction terms between the adversaries: if y increases their resources then x will increase at a rate of b_1 and if x increases their resources then y will increase at a rate of b_2. The $a_1 x$ and $a_2 y$ terms reflect some form of economic fatigue or cost associated with growing resources: the larger the number of resources, the higher the cost. The c_1 and c_2 terms are external 'grievances' for x and y respectively, which represent growth or reduction in resources at a constant rate, due to external factors.

These equations model the evolution of the number of resources (traditionally arms) belonging to two adversaries who react to one another by means of an action-reaction relationship. That is, if x acts to increase its arms, y will react to this and increase its own arms, subject to some economic cost-benefit calculation that depends on the parameters in (14). The two-dimensional system has one equilibrium point, where neither x nor y opt to increase their levels of arms. This equilibrium point can be calculated as

$$(x_e, y_e) = \left(\frac{c_1 a_2 + c_2 b_1}{a_1 a_2 - b_1 b_2}, \frac{b_2 c_1 + a_1 c_2}{a_1 a_2 - b_1 b_2} \right), \tag{15}$$

which exists, and lies in the positive quadrant (*i.e.* for levels of arms greater than zero), when all parameters are greater than zero and $a_1 a_2 > b_1 b_2$, which is to say that the economic fatigue parameters outweigh the competition parameters in the action-reaction dynamics. It can also be shown that the equilibrium is globally stable when $a_1 a_2 > b_1 b_2$

and so, in this situation, all trajectories of arms will converge to the point (15). If the competition terms outweigh the economic fatigue, so that $b_1 b_2 > a_1 a_2$, the equilibrium is no longer stable and solutions diverge towards infinity in the positive quadrant (since the equilibrium is in the negative quadrant). This behaviour corresponds to an 'arms race', or conflict escalation more generally. These simple results confirm our intuition that escalation may occur when two adversaries are only lightly affected by economic constraints but are strongly competitive.

In a spatial model of conflict escalation, we are interested in the change in the number of resources of each team within each zone. We therefore require expressions for $\dot{x}_i$ and $\dot{y}_i$. Following Richardson, we require an action-reaction term that causes a team to adjust its numbers of resources in response to the number of resources of its opponent. Since this is a spatial model, we are interested in the distribution of an opponent's arms. We therefore let the action-reaction term be proportional to the measure of threat on a team that we derived in section 2. Extending the other terms to the Richardson equation in the obvious way, we derive the spatial extension to Richardson's model of conflict escalation:

$$\begin{aligned} \dot{x}_i &= b_1 \tau_i^x - a_1 x_i + c_1 \\ \dot{y}_i &= b_2 \tau_i^y - a_2 y_i + c_2, \end{aligned} \tag{16}$$

for zones $i = 1, 2, 3, ..., N$.

3.1 Relationship to the original Richardson model

The spatial extension to the Richardson model is obtained by embedding a measure of spatially-dependent threat into the dynamics. The parameter β determines the degree of spatial influence on this measure of threat, as is evident when the full system of $2N$ non-linear differential equations is presented as:

$$\begin{aligned} \dot{x}_i &= -a_1 x_i + b_1 h_x \sum_j \frac{y_j x_i e^{-\beta d_{ij}}}{\sum_k x_k e^{-\beta d_{kj}}} + c_1 \\ \dot{y}_i &= -a_2 y_i + b_2 h_y \sum_j \frac{x_j y_i e^{-\beta d_{ij}}}{\sum_k y_k e^{-\beta d_{kj}}} + c_2. \end{aligned} \tag{17}$$

As $\beta \to \infty$, the cost to exert threat on any zone other than one's own becomes infinite. To leading order, the influence of a player's adversaries in surrounding zones becomes negligible and all zones become isolated. In this case, the system reduces to N decoupled versions of the original Richardson model, one for each zone. It is straightforward to demonstrate this analytically by considering (17) as $\exp(-\beta) = \delta \to 0$.

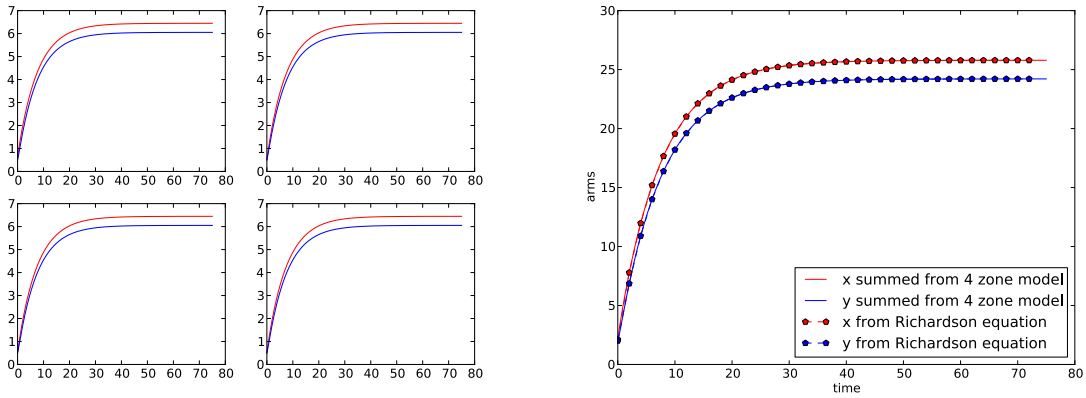

(a) (b)

Figure 2: Demonstrating that when $\beta = 0$, the aggregate arms over the zone structure follows that of the original Richardson system. The parameters used are $(a_1, b_1, c_1, h_x, a_2, b_2, c_2, h_y) = (-1, 0.9, 1, 1, -0.5, 1.8, 0.5, 1)$, the initial conditions are $x_i, y_i = 0.5$ everywhere, except in zone 1, where $x_1 = 0.6$.

Similarly, when $\beta = 0$, all zones have equal influence on one another, independent of the distance which separates them. In this case, the aggregate solution will follow the original Richardson dynamics. This can be shown by summing the evolution equation for x and y across all zones:

$$\sum_{i=1}^{N} \dot{x}_i = -a_1 \sum_{i=1}^{N} x_i + b_1 \sum_{i=1}^{N} x_i \left(\frac{\sum_{j=1}^{N} y_j}{\sum_{k=1}^{N} x_k} \right) + N c_1, \tag{18}$$
$$\sum_{i=1}^{N} \dot{y}_i = -a_2 \sum_{i=1}^{N} y_i + b_2 \sum_{i=1}^{N} y_i \left(\frac{\sum_{j=1}^{N} x_j}{\sum_{k=1}^{N} y_k} \right) + N c_2,$$

and using the shorthand notation $\sum_{i=1}^{N} x_i = X$, $\sum_{i=1}^{N} y_i = Y$. This gives

$$\dot{X} = -a_1 X + b_1 h_x Y + N c_1, \tag{19}$$
$$\dot{Y} = -a_2 Y + b_2 h_y X + N c_2$$

and the similarities to (14) are clear. Figure 2 confirms this result numerically, where the sum of the arms in a four zone model (see section 4.3) are compared with (19).

For $\beta > 0$, the effect of β (other than as a measure of spatial influence) is interdependent with the parameters a, b, c, d_{ij}. In the following section we investigate how these parameters affect the qualitative behaviour of the system. As well as improving our understanding of the model, insights here may inform the choice of parameters for various applications.

4 Analysis of the spatial Richardson model

Initial observations suggest that the non-linear spatial Richardson model in (17) cannot be solved analytically. Numerical simulations of the model may therefore give insights into the system dynamics. We firstly reduce the number of parameters under consideration, and then attempt to isolate the effects of those remaining.

Firstly, note that by setting $\bar{b_1} = b_1 h_x$ and then relabelling $\bar{b_1}$ as b_1, and similarly for b_2, we can remove the need for parameters h_x and h_y.

Secondly, assuming that $a_1 = a_2 = a$, and substituting

$$t = \frac{1}{a}\hat{t}, \qquad b_i = a\hat{b}_i, \qquad c_i = a\hat{c}_i, \tag{20}$$

into (16), it can be shown that a may be eliminated. For a system with time-scale $\hat{t}$, it is sufficient to take $a = 1$. For the original system, a has no effect on the qualitative behaviour; it is equivalent to scaling the time in which dynamics occur.

Removing these parameters, and dropping hats for ease of notation, the system is:

$$\begin{aligned} \dot{x_i} &= b_1 \sum_j \frac{y_j x_i e^{-\beta d_{ij}}}{\sum_k x_k e^{-\beta d_{kj}}} - x_i + c_1 \\ \dot{y_i} &= b_2 \sum_j \frac{x_j y_i e^{-\beta d_{ij}}}{\sum_k y_k e^{-\beta d_{kj}}} - y_i + c_2. \end{aligned} \tag{21}$$

For simulations of the system, temporal discretisation has been achieved using Euler's method:

$$\begin{aligned} x_i(t+\delta t) &= x_i(t) + \delta t \left(b_1 \sum_j \frac{y_i(t) x_j(t) e^{-\beta d_{ij}}}{\sum_k x_k(t) e^{-\beta d_{ik}}} - x_i(t) + c_1 \right) \\ y_i(t+\delta t) &= y_i(t) + \delta t \left(b_2 \sum_j \frac{x_i(t) y_j(t) e^{-\beta d_{ij}}}{\sum_k y_k(t) e^{-\beta d_{ik}}} - y_i(t) + c_2 \right). \end{aligned} \tag{22}$$

This approximation is equivalent to the model (21) in the limit $\delta t \to 0$. Thus it is necessary to pick δt, on one hand, small enough for accurate simulations, but on the other, large enough for computational viability. It was found that consistent solutions arose for values of $\delta t < 0.05$.

It was discovered in early simulations that several bifurcations exist as the parameters vary. It is possible to derive analytical expressions for the points of bifurcation, and to explain why they occur, for small numbers of zones. For this reason, we restrict this section to consideration of a two-zone system with distance matrix

$$d_{ij} = \begin{cases} 0 & \text{if } i = j, \\ 1 & \text{if } i \neq j. \end{cases} \tag{23}$$

	Value of b	Observed large time behaviour
Case 1:	$0 \leq b < B$	Steady state of $x_1 = y_1 = x_2 = y_2$.
Case 2:	$B < b < 1$	Steady state of $x_1 = y_1$ and $x_2 = y_2$ although $x_1, y_1 > x_2, y_2$.
Case 3:	$b = 1$	$x_1 = y_1$ grow linearly with time, $x_2 = y_2$ reach a steady state.
Case 4:	$1 < b < e^{\beta}$	$x_1 = y_1$ grows exponentially with time, $x_2 = y_2$ reach a steady state.
Case 5:	$b = e^{\beta}$	$x_1 = y_1$ grows exponentially with time, $x_2 = y_2$ grows linearly.
Case 6:	$b > e^{\beta}$	$x_1 = y_1$ and $x_2 = y_2$ both grow exponentially with time.

Figure 3: Summary of the bifurcation points and large time behaviour of the special case outlined in section 4.1

It is worth noting at this stage that these results can theoretically be extrapolated to all zone structures; however, a small increase in the number of zones dramatically increases the analytical intractability of the system. Some examples of different zone structures are given in section 4.3.

For the purpose of this section, we fix $b_1 = b_2 = b$ and $c_1 = c_2 = c$, and use initial conditions:

$$x(t=0) = \begin{pmatrix} 0.6 \\ 0.5 \end{pmatrix}, \qquad y(t=0) = \begin{pmatrix} 0.5 \\ 0.5 \end{pmatrix}, \tag{24}$$

where $x_1 = 0.6$ is chosen to avoid resting on the conditionally unstable steady state equilibrium of all arms equal in all zones.

4.1 The effect of b and c

Using the model setup outlined above, it was found that, when varying b, the system exhibits several transitions of qualitative behaviour. These bifurcations take place at the values $b = B, 1, e^{\beta}$, where B is a value between 0 and 1. Either side of and at these points, the observed behaviour is summarised in the table in Figure 3, and analysis of each of the cases is given in the following sections.

It was also found that the value of c had no qualitative effect on the model, instead c affects the value of any steady states, and the rates of linear growth, as becomes clear in the rest of this section.

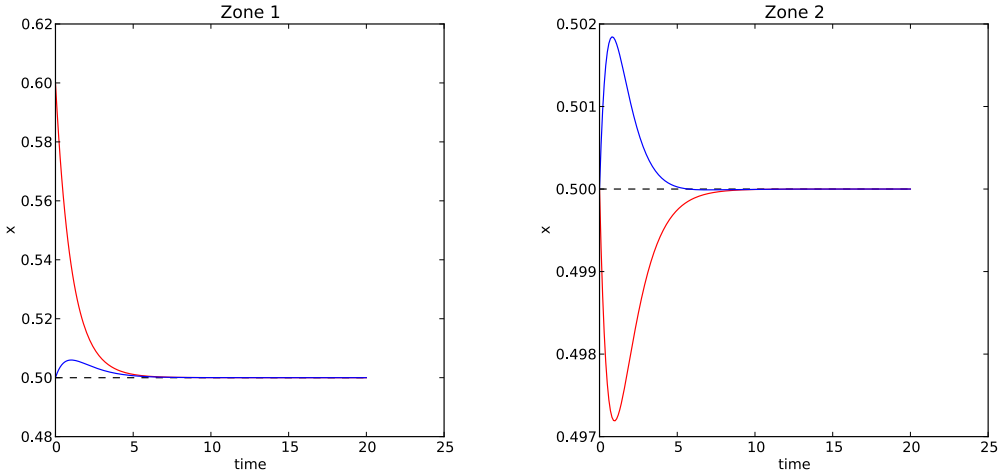

Figure 4: (Case 1) all zones settle to an equilibrium value given by $\frac{c}{1-b}$. In this case, $b = 0.6$ and $c = 0.4$.

4.1.1 Case 1: $0 \leq b < B$

In this case, the arms in both zones, and for both teams, converge to a single equilibrium value. To determine the value of this equilibrium analytically, the proposed value, X can be substituted into the dynamic equations and the rate of change set to zero. The equations in this case, which are identical for all zones and teams, are then given by:

$$0 = -X + b\left(\frac{X^2}{X + Xe^{-\beta}} + \frac{X^2 e^{-\beta}}{X + Xe^{-\beta}}\right) + c, \tag{25}$$

with unique solution

$$X = \frac{c}{1-b}. \tag{26}$$

Numerical simulations which demonstrate this behaviour can be seen in Figure 4. Also plotted as a dashed line is the value given in (26), demonstrating that the arms in all zones do indeed converge to that value.

The stability of this solution may be analysed by examining the eigenvalues of the Jacobian of the system. By setting

$$f_1 = -x_1 + bx_1\left(\frac{y_1}{x_1 + x_2 e^{-\beta}} + \frac{y_2 e^{-\beta}}{x_1 e^{-\beta} + x_2}\right) + c, \tag{27}$$

and f_2, g_1, g_2 as the equivalent expressions for x_2, y_1, y_2, the system will be in a steady state whenever $f_1 = f_2 = g_1 = g_2 = 0$. The Jacobian of such a system is given by:

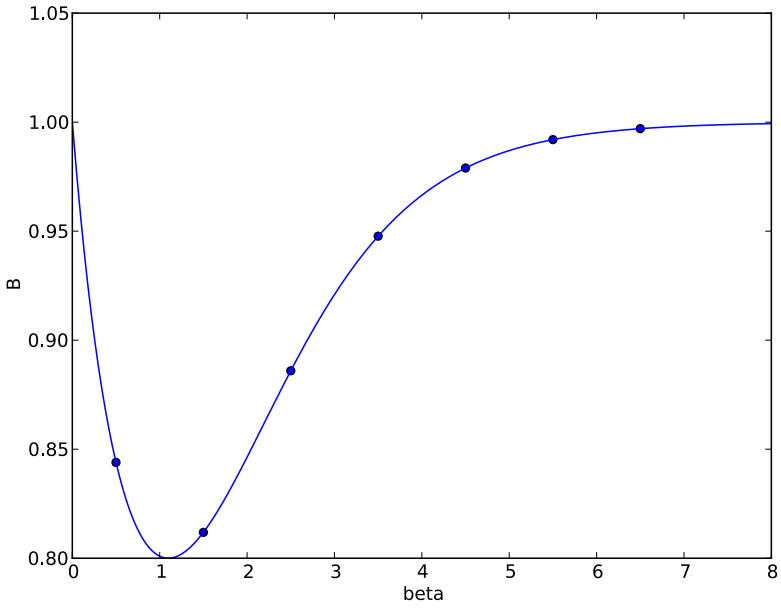

Figure 5: The bifurcation point as in (31) as a blue line, versus some numerical simulations to determine the point at which (26) becomes unstable as blue circles.

$$J = \begin{pmatrix} \frac{\partial f_1}{\partial x_1} & \frac{\partial f_1}{\partial x_2} & \frac{\partial f_1}{\partial y_1} & \frac{\partial f_1}{\partial y_2} \\ \\ \frac{\partial f_2}{\partial x_1} & \frac{\partial f_2}{\partial x_2} & \cdots & \frac{\partial f_2}{\partial y_2} \\ \vdots & \vdots & \ddots & \vdots \\ \frac{\partial g_2}{\partial x_1} & \cdots & \cdots & \frac{\partial g_2}{\partial y_2} \end{pmatrix} \tag{28}$$

and in general will be a $2N$x$2N$ matrix, which highlights the difficulty of carrying out analytical investigations for a model including any more than two zones.

The four eigenvalues of (28), when the system is in the equilibrium state outlined in (26), are calculated to be:

$$\begin{aligned} \lambda_1 &= -b-1 & \lambda_2 &= b-1 \\ \lambda_3 &= \tfrac{4be^{\beta}+be^{2\beta}-b-2e^{\beta}-e^{2\beta}-1}{\left(e^{\beta}+1\right)^2} & \lambda_4 &= -\tfrac{-4be^{\beta}+be^{2\beta}-b+2e^{\beta}+e^{2\beta}+1}{\left(e^{\beta}+1\right)^2} \end{aligned} \tag{29}$$

where, for brevity, we choose not to include more detail of our derivation. The equilibrium is stable when all the eigenvalues have negative real part. Thus, we find four conditions

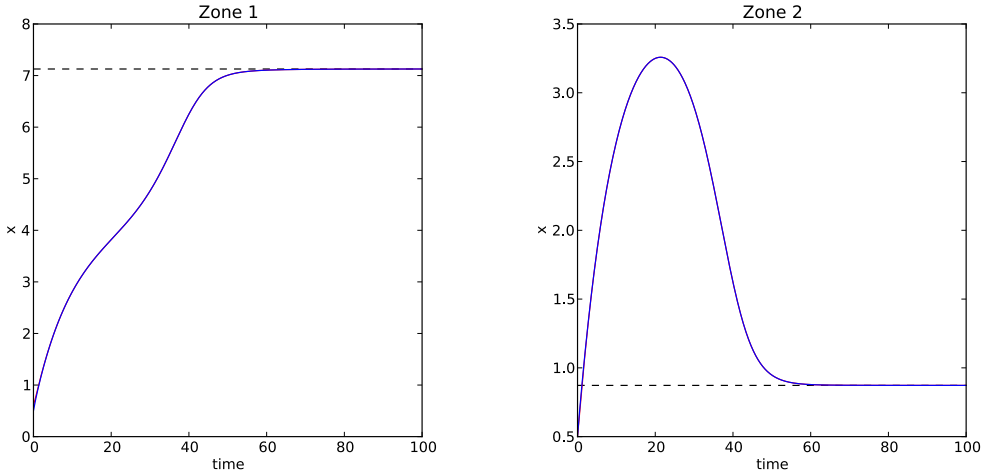

Figure 6: (Case 2) All zones settle to an equilibrium value, but the level of arms in zone 1 is greater than that in zone 2.

on b for the stability of an all-equal system:

$$\begin{array}{ll} b > -1 & b < 1 \\ b < \frac{\left(e^{\beta}+1\right)^2}{4e^{\beta}+e^{2\beta}-1} & b < \frac{\left(e^{\beta}+1\right)^2}{4e^{\beta}-e^{2\beta}+1} \end{array} \tag{30}$$

Given that b must be positive, the first condition is always satisfied. In addition, the second and fourth conditions are bounded below by the third, and are always satisfied here. It is therefore the third condition which indicates stability of this solution, and hence gives us our first bifurcation point, and the value of B.

$$B = \frac{\left(e^{\beta}+1\right)^2}{4e^{\beta}+e^{2\beta}-1}. \tag{31}$$

The stability of the solution (26) may be tested numerically to verify our findings. Since decimals are represented as binary fractions, if a simulation is run to very large times, small numerical errors accumulate and can act to knock the system off an unstable equilibrium position. In Figure 5, we plot the value of b at which the solution (26) becomes unstable, for various values of β. On the same figure, we plot the analytical expression in (31) for varying β. This confirms that (31) is the bifurcation point.

4.1.2 Case 2: $B < b < 1$

As b increases past B, the behaviour in zone 1 diverges from that in zone 2, and the system settles to an equilibrium for which $x_1 = y_1$ and $x_2 = y_2$, but $x_1, y_1 > x_2, y_2$, as can be seen in Figure 6. Numerical simulations also suggest that this equilibrium is stable

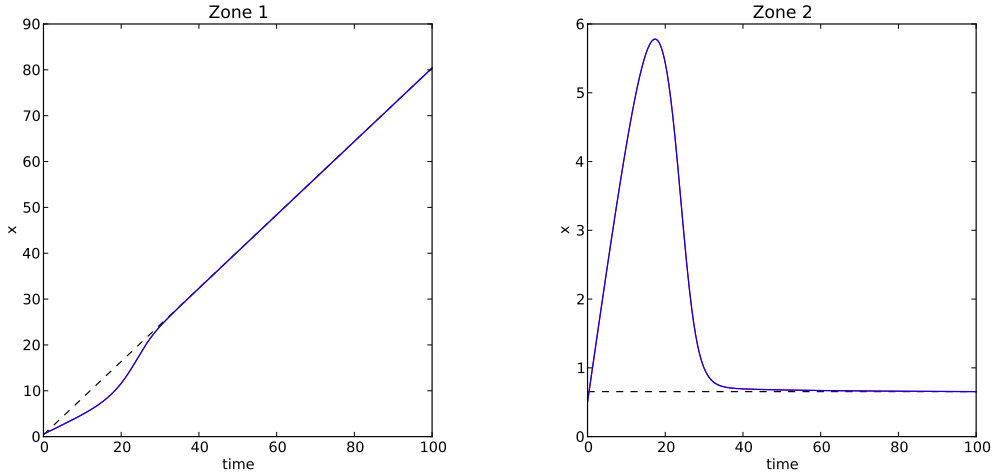

Figure 7: (Case 3) Arms levels in zone 1 no longer settle to an equilibrium as before, but now increase linearly with gradient $2c$, whilst zone 2 settles to a constant level of $\frac{c}{1-e^{-\beta}}$.

when subjected to perturbations, although we are yet to derive an analytic explanation of this behaviour. Simulations also suggest that this solution becomes unstable at $b = 1$; the behaviour at this point is discussed in the following section.

It is worth noting that as $\beta \to 0$ or $\beta \to \infty$, $B \to 1$, and the width of the interval in b for which this case applies, shrinks. Therefore, space must have an influence on the model for zones to reach a steady state with different arms in each zone.

4.1.3 Case 3: $b = 1$

When b reaches 1, the level of arms in zone 1 no longer converges to an equilibrium. After an initial transient stage, the arms level in this zone increases linearly with gradient $2c$ (in the general, n-zone case, this value is given by nc), whilst zone 2 settles to an equilibrium (when more zones are added, they also converge to this value). This behaviour, and the gradient of arms increase in zone 1, can be derived analytically by substituting into the equations an equilibrium value of X_2 for zone 2 and a gradient of m for zone 1:

$$m = -x_1 + b\left(\frac{{x_1}^2}{x_1 + X_2 e^{-\beta}} + \frac{x_1 X_2 e^{-\beta}}{x_1 e^{-\beta} + X_2}\right) + c \tag{32}$$

$$0 = -X_2 + b\left(\frac{x_1 X_2 e^{-\beta}}{x_1 + X_2 e^{-\beta}} + \frac{{X_2}^2}{x_1 e^{-\beta} + X_2}\right) + c \tag{33}$$

Since the behaviour we are seeking involves linear growth in x_1, these equations should also hold true in the limit as $x_1 \to \infty$. Taking this limit in (33) and using $b = 1$ gives

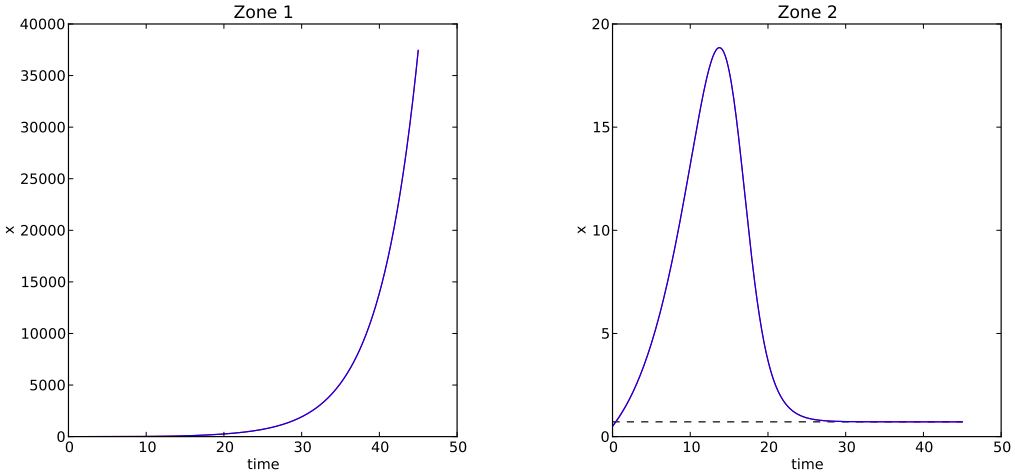

Figure 8: (Case 4) Arms levels in zone 1 increase exponentially, but zone 2 settles to an equilibrium at $\frac{c}{1-be^{-\beta}}$

the value for X_2:

$$0 = X_2(e^{-\beta} - 1) + c$$
$$X_2 = \frac{c}{1 - e^{-\beta}} \tag{34}$$

which can then be substituted into (32), after re-arranging and taking the limit:

$$m = 2c \tag{35}$$

This behaviour can be seen in Figure 7.

4.1.4 Case 4: $1 < b < e^{\beta}$

If b is increased above 1, the 'linear growth' solution above is no longer possible. For $b \neq 1$, the right-hand-side of equation (32) becomes:

$$\frac{(b-1){x_1}^2}{x_1 + X_2 e^{-\beta}} + \frac{x_1 X_2 e^{-\beta}}{x_1 + X_2 e^{-\beta}} + \frac{x_1 X_2 e^{-\beta}}{x_1 e^{-\beta} + X_2} + c$$

the first term of which will cause exponential growth of x_1 in the limit to ∞ and therefore preclude a linear solution. The analysis for zone 2, however, still stands, with equation (33) now having become:

$$0 = -X_2 + b\left(\frac{x_1 X_2 e^{-\beta}}{x_1 + X_2 e^{-\beta}} + \frac{{X_2}^2}{x_1 e^{-\beta} + X_2}\right) + c \tag{36}$$

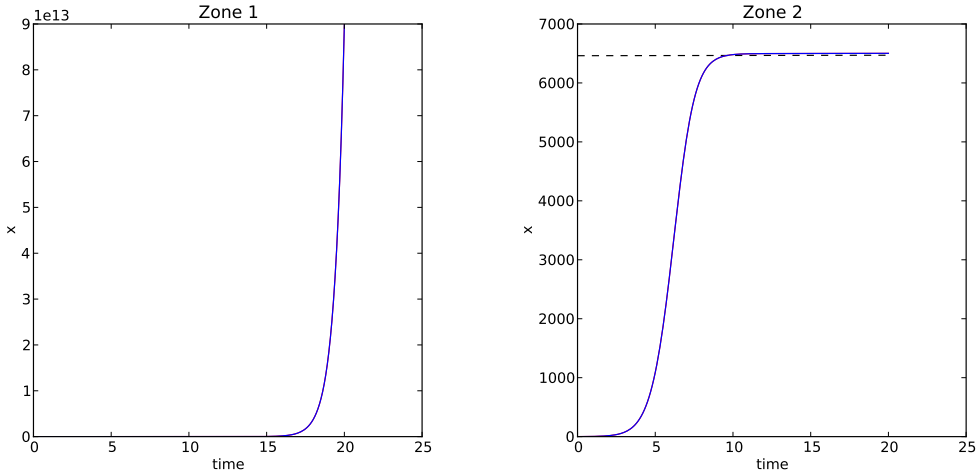

Figure 9: (Case 5) Zone 1 shows exponential growth, but arms levels in zone 2 now grow linearly with gradient c.

which, in the limit as $x_1 \to \infty$, reduces to:

$$0 = X_2(be^{-\beta} - 1) + c$$
$$X_2 = \frac{c}{1 - be^{-\beta}} \tag{37}$$

Indeed this behaviour - exponential increase in zone 1 and steady state in zone 2 - is observed in the numerical simulations, and can be seen in Figure 8.

4.1.5 Case 5: $b = e^{\beta}$

Clearly the condition of equation (37) becomes undefined at $b = e^{\beta}$ and therefore a steady state for x_2 is no longer possible. Still, however, seeking a solution where $x_1 \to \infty$, the equation for behaviour in zone 2 reduces to:

$$\dot{x_2} = x_2(be^{-\beta} - 1) + c \tag{38}$$
$$\dot{x_2} = c \tag{39}$$

and we therefore have linear growth with gradient c in zone 2 (and other zones, for an n-zone model) to go with the exponential growth in zone 1. A simulation showing such behaviour can be seen in Figure 9.

4.1.6 Case 6: $b > e^{\beta}$

If b is at a level greater than e^{β}, consideration of the dynamical equations in the limit to ∞ now show clearly that solutions with constant growth rate are impossible; equation

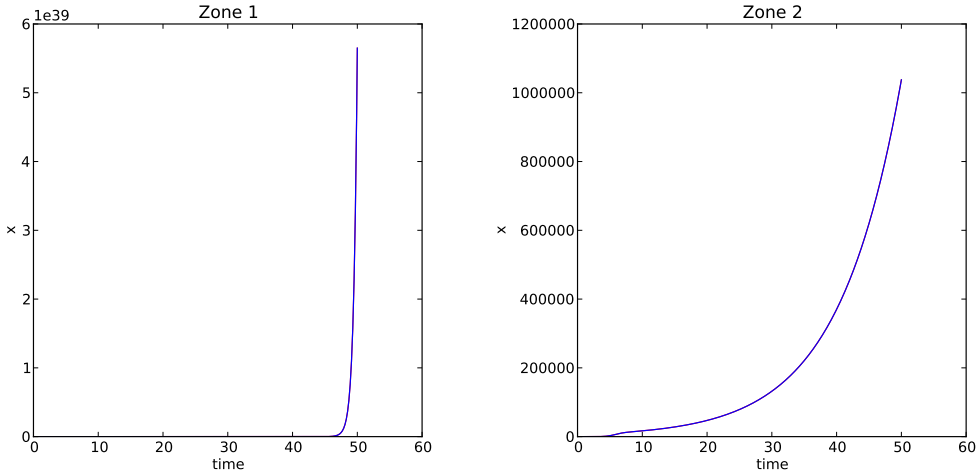

Figure 10: (Case 6) Exponential growth of arms in both zones.

(38), for example, is dominated by x_2 and will lead to exponential growth in zone 2 also. This behaviour is shown in Figure 10.

4.2 The effect of β

Beyond the relationship between β and b outlined in case 1, it is possible to find special cases where β serves only to affect the timescale of the problem, as can be seen in the example shown in figure (11) .

The plots in Figure 11 all appear to settle on the same steady state, suggesting that the steady state solution in this special case is independent of β. However, the time taken to reach this steady state varies across the images, where (f) has not yet settled by $t = 100$. The graphs appear to suggest that the timescale of the problem is dependent on beta. Indeed, the time it takes for the system to reach a steady state may be plotted against β and is shown in Figure 12. Here we see a smooth relationship with a minimum at around $\beta = 1.8$. Although the plot appears to suggest an analytic relationship between the two, in our early investigations we were not able to derive such an expression.

Although special cases and examples such as this may be found and explored, the full influence of β on the dynamics is, generally speaking, hidden within the non-linearities of the system and remains an issue which we would be keen to investigate in the future.

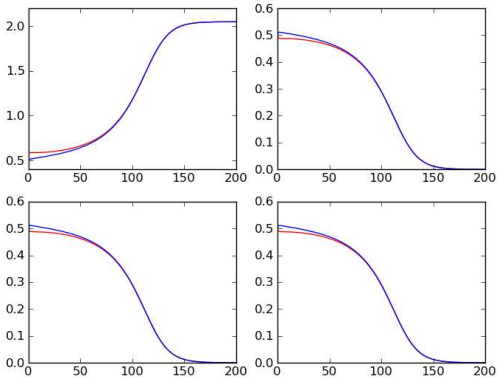

(a) $\beta = 0.1$

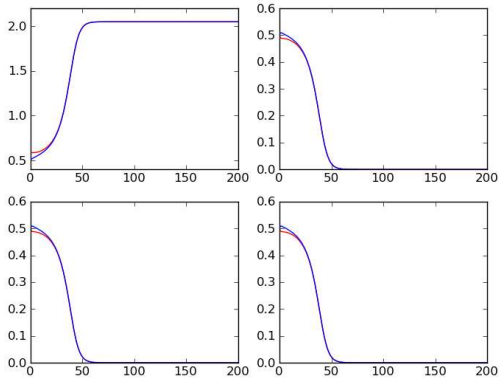

(b) $\beta = 0.3$

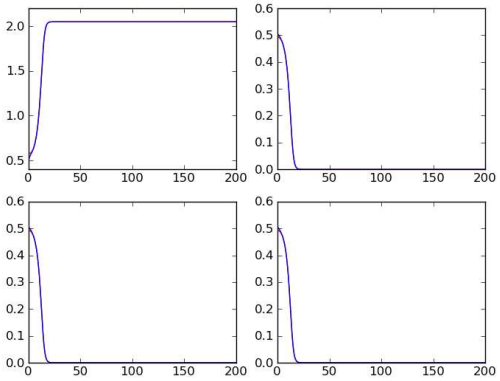

(c) $\beta = 1.5$

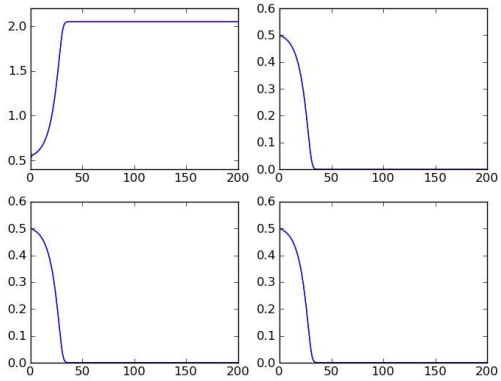

(d) $\beta = 3.2$

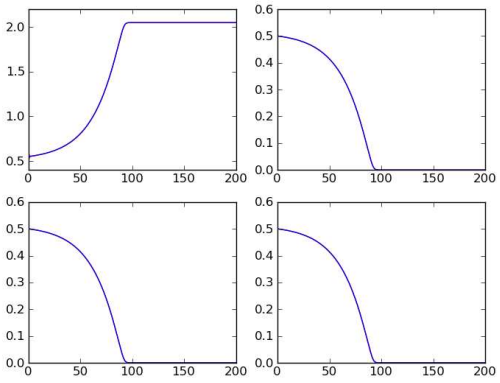

(e) $\beta = 4.5$

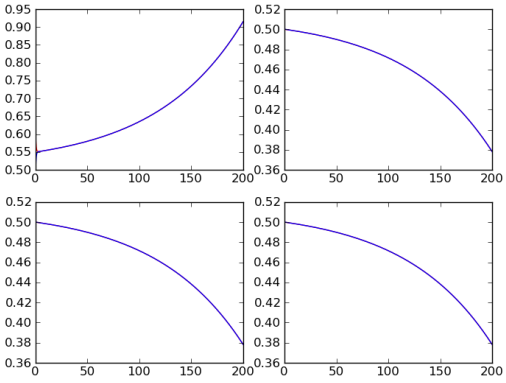

(f) $\beta = 5.8$

Figure 11: A special case where β effects only the timescale of the problem. The parameters are $(a_1, b_1, c_1, a_2, b_2, c_2) = (-1, 1, 0, -1, 1, 0)$ with initial conditions as in (24)

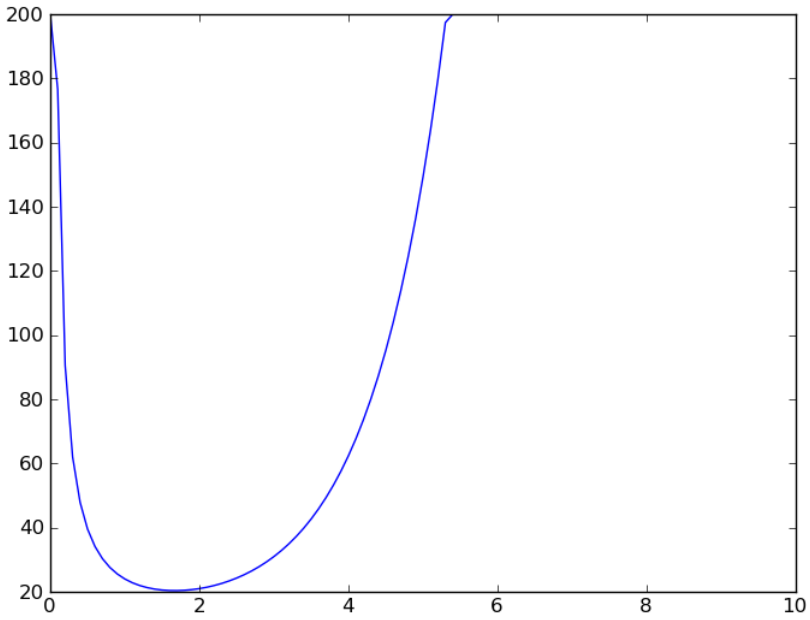

Figure 12: The time taken to reach equilibrium as β varies.

4.3 The effect of d_{ij}

In this section, in order to investigate the effect of the distance matrix d_{ij}, the number of zones under consideration is increased to four. The above analysis for two zones may be extrapolated to the four zone case when the distance matrix is defined similarly and given by:

$$d = \begin{pmatrix} 0 & 1 & 1 & 1 \\ 1 & 0 & 1 & 1 \\ 1 & 1 & 0 & 1 \\ 1 & 1 & 1 & 0 \end{pmatrix}, \tag{40}$$

for which the arrangement of zones can be thought of as in Figure 13(a), where the cost of impedance across all zones is equal. The plots in Figure 13 show the evolution of the four zone system for different values of b. These examples use the parameters:

$$a_1 = a_2 = -1 \tag{41}$$

$$b_1 = b_2 = b \tag{42}$$

$$c_1 = c_2 = 0.1 \tag{43}$$

$$\beta = 1, \tag{44}$$

with initial conditions $x_1 = 0.6$ and $x_i = y_i = 0.5$ for all other i, where, again, initial conditions were chosen to simulate a perturbation in the first zone in order to avoid resting on an initial unstable equilibrium (with all arms equal in all zones). For the remainder of this section, these parameters are used. For the arrangement of zones given by the matrix (40), numerical simulations appear to suggest that not only does the evolution of the four-zone case behave in a similar way to the two-zone analysis performed in section 4.1, for different values of b, but also that bifurcations in the qualitative behaviour of the model occur at similar locations in the parameter space.

By varying the matrix in (40), it is possible to consider different arrangements of zones. By doing this, we gain intuition on how the model behaves, and are able to investigate the effect of space. As an example, consider the cost matrix given by

$$d = \begin{pmatrix} 0 & 1 & 10 & 100 \\ 1 & 0 & 1 & 10 \\ 10 & 1 & 0 & 1 \\ 100 & 10 & 1 & 0 \end{pmatrix}, \tag{45}$$

which can be thought of as the arrangement of zones in Figure 14(a), where the distance between two zones increases by an order of magnitude as the zones become further separated from one another. Figure 14 shows the evolution of this system for different values of b. For $b = 0.8$ the number of arms in zones 2 and 3 rises, whilst the arms in zones 1 and 4 decrease. This is different to the case with distance matrix (40) as this equilibrium value has different levels of arms in each zone. The level of arms rises in the zones in the centre of the arrangement, due to the lower impedance of delivering threat to these zones; these simulations therefore suggest that zones which are most accessible will experience a higher level of arms. The equilibrium appears to be stable in numerical perturbation tests. In this example, the spatial structure of the zone layout has a significant effect on the dynamics of the system.

In the second case, where $b = 0.9$, the systems finds a new equilibrium which is different to the case for $b = 0.8$. In contrast to the two-zone case, the zone with the highest level of arms is not the zone in which the initial perturbation took place, but rather the zone which is closest to the initial perturbation, but still in a position with overall high accessibility.

For the case of $b \geq 1$, there is an arms race occurring in zone 2 for the same reason. In order for arms races to occur in any of the other zones, b must be increased above e^{β}.

A further example demonstrates how this behaviour generalises to other shapes. In

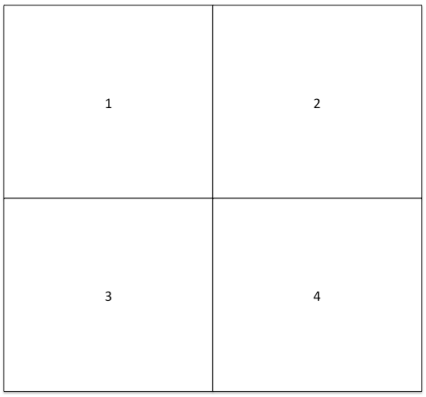

(a) Zone arrangement for the distance matrix in (40). The cost of delivering threat diagonally is equal to the cost of delivering threat horizontally or vertically.

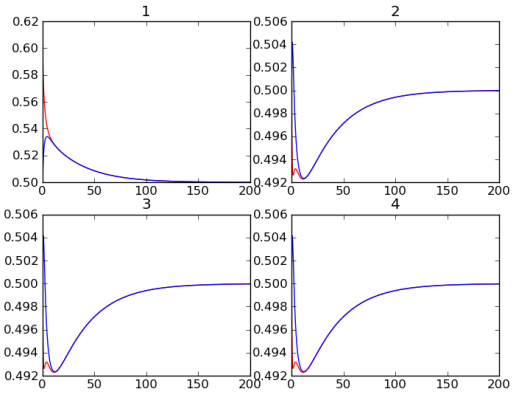

(b) $b = 0.8$

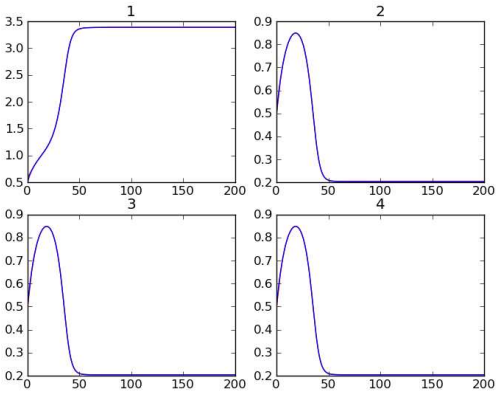

(c) $b = 0.9$

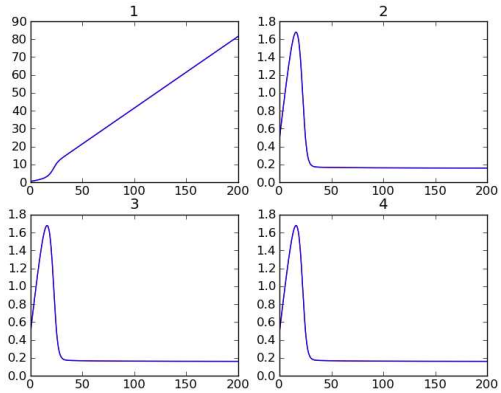

(d) $b = 1.0$

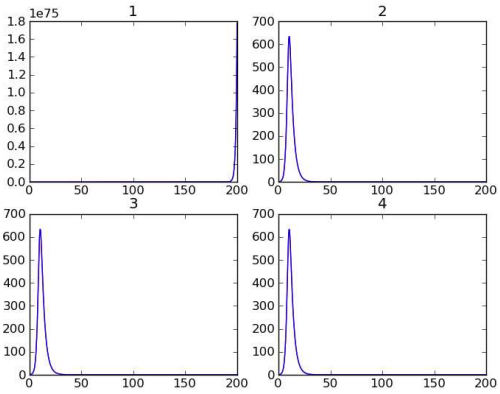

(e) $b = 1.5$

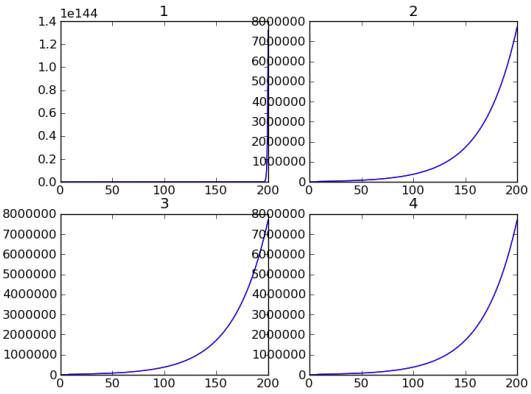

(f) $b = 2.8$

Figure 13: Results for various b values for the arrangement of zones in (a).

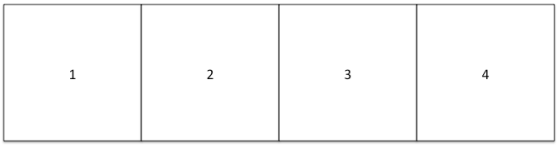

(a) Zone arrangement for the distance matrix in (45).

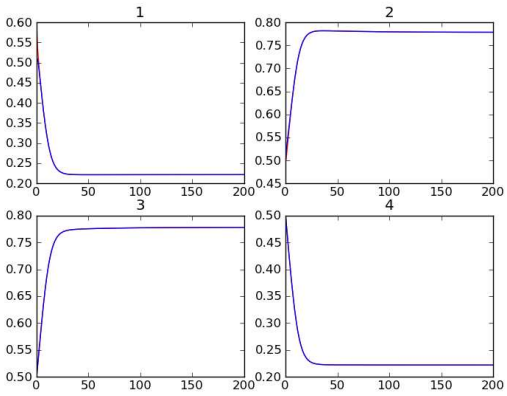

(b) $b = 0.8$

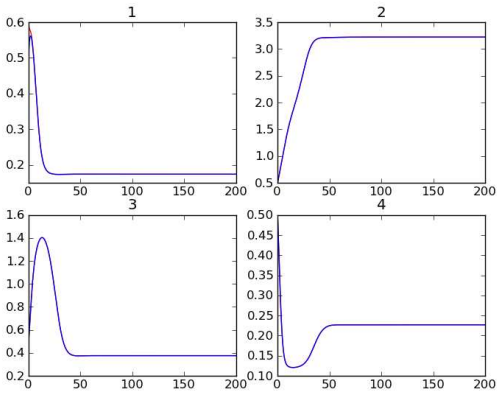

(c) $b = 0.9$

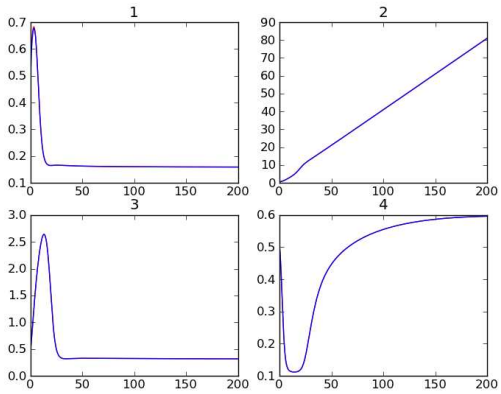

(d) $b = 1.0$

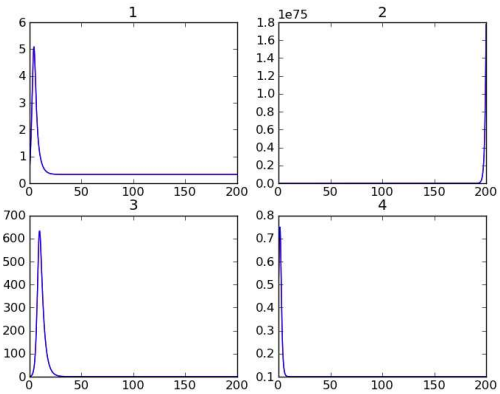

(e) $b = 1.5$

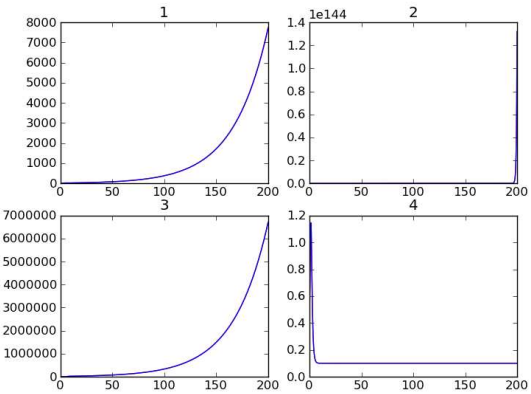

(f) $b = 2.8$

Figure 14: Results for various b values for the arrangement of zones in (a).

this case, we keep all parameters the same but set the distance matrix to:

$$d = \begin{pmatrix} 0 & 1 & 10 & 1 \\ 1 & 0 & 1 & 1 \\ 10 & 1 & 0 & 1 \\ 1 & 1 & 10 & 0 \end{pmatrix}, \tag{46}$$

so that the zones can be thought of as being in the arrangement shown in Figure 15(a). The results for simulations for different values of b are shown in Figure 15. Again, the most volatile zone (the one with the highest level of arms or most likely to result in an arms race) is the one which is most accessible from all of the other zones.

5 A border dispute

In this section, we present an example of a border dispute to demonstrate just one possible application of the model described and analysed in sections 3 and 4. This example also indicates how the model might be implemented in a real-world situation. Suppose two adversaries have resources distributed over a finite number of points, which may be military bases or outposts. A discrete zone structure can be derived from these points, using a Voronoi diagram. Figure 16 shows a Voronoi diagram where the zones are coloured according to which team that zone is occupied by. The map in Figure 16 can be considered as a border between two adversaries. The distance matrix d_{ij} is calculated as the distance between the centres which gave rise to the Voronoi map or, equivalently, the distance between each military base.

Figure 17 shows the outcome of a simulation of this system using parameters $beta = 1$, $a_1 = a_2 = 1$, $b_1 = b_2 = 0.9$, $c_1 = c_2 = 0.8$ and with initial arms randomised in the interval $(0, 1)$. The simulated results show that the most volatile zones (*i.e.* zones with highest number of arms) are, in general, those closest to the border.

This example demonstrates how this model can be applied to a real-world situation. Real-world geo-political topographies may be incorporated into the distance matrix, where the cost of impedence may include measures of geographical features. Careful consideration of parameters may allow analysis of military disputes where space is considered explicitly.

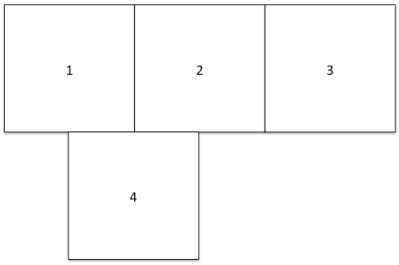

(a) Zone arrangement

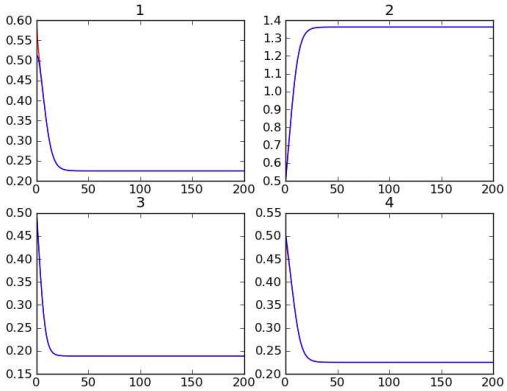

(b) $b = 0.6$

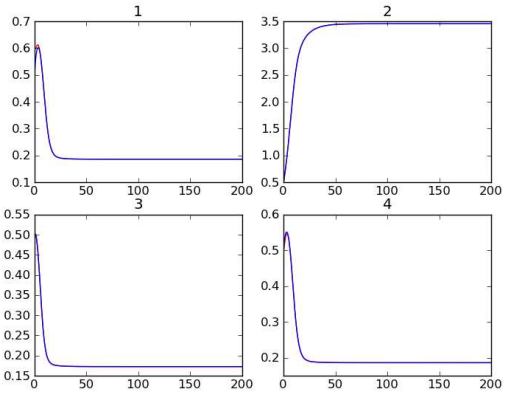

(c) $b = 0.8$

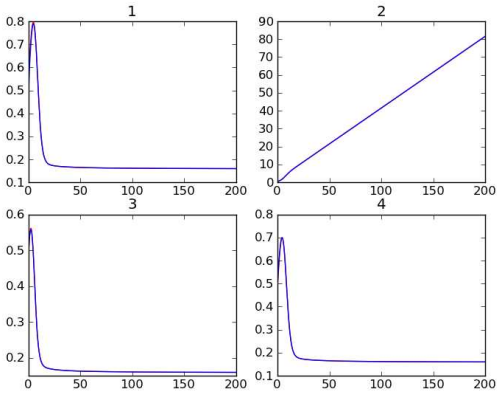

(d) $b = 1.0$

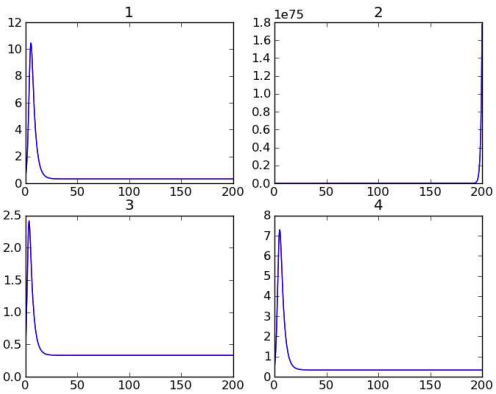

(e) $b = 1.9$

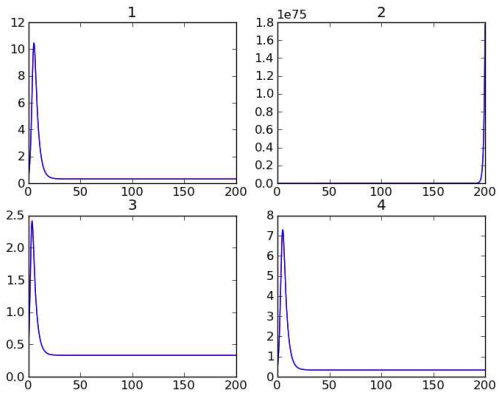

(f) $b = 2.8$

Figure 15: Results for various b values for the zone arrangement given by the distance matrix in (46)

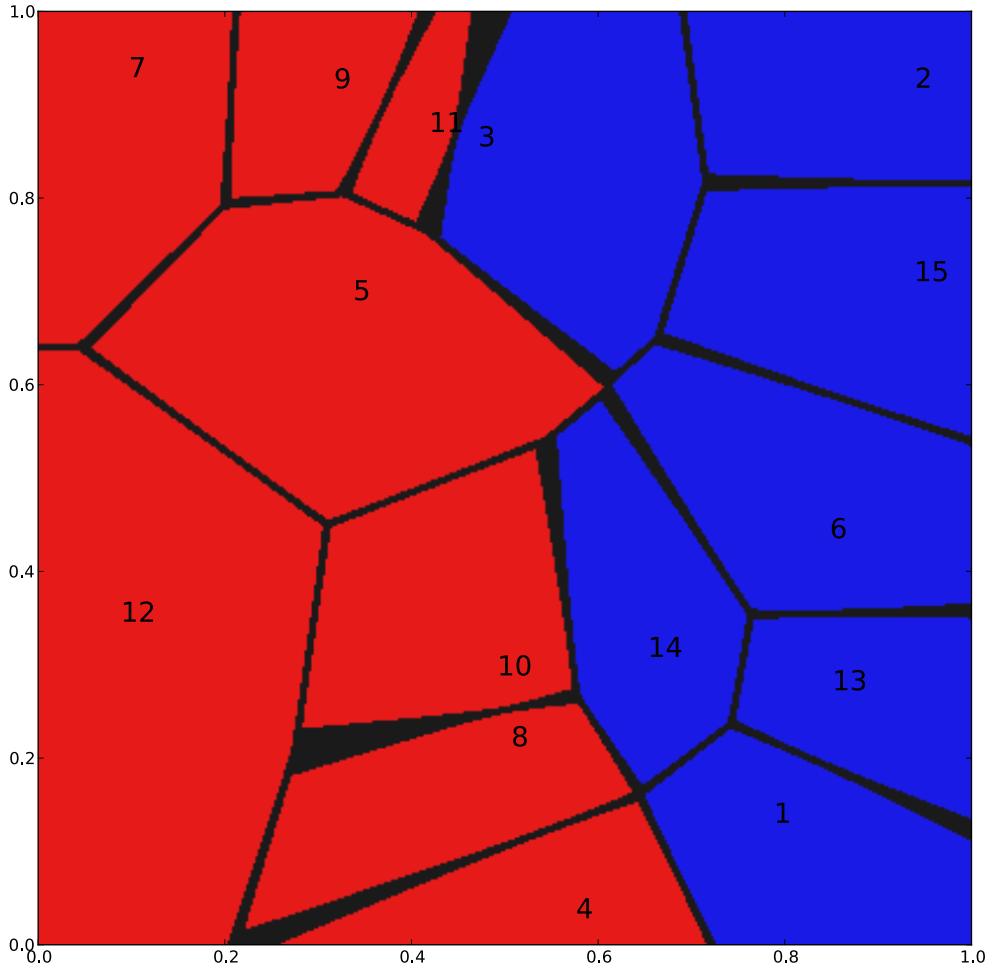

Figure 16: Voronoi map for the given

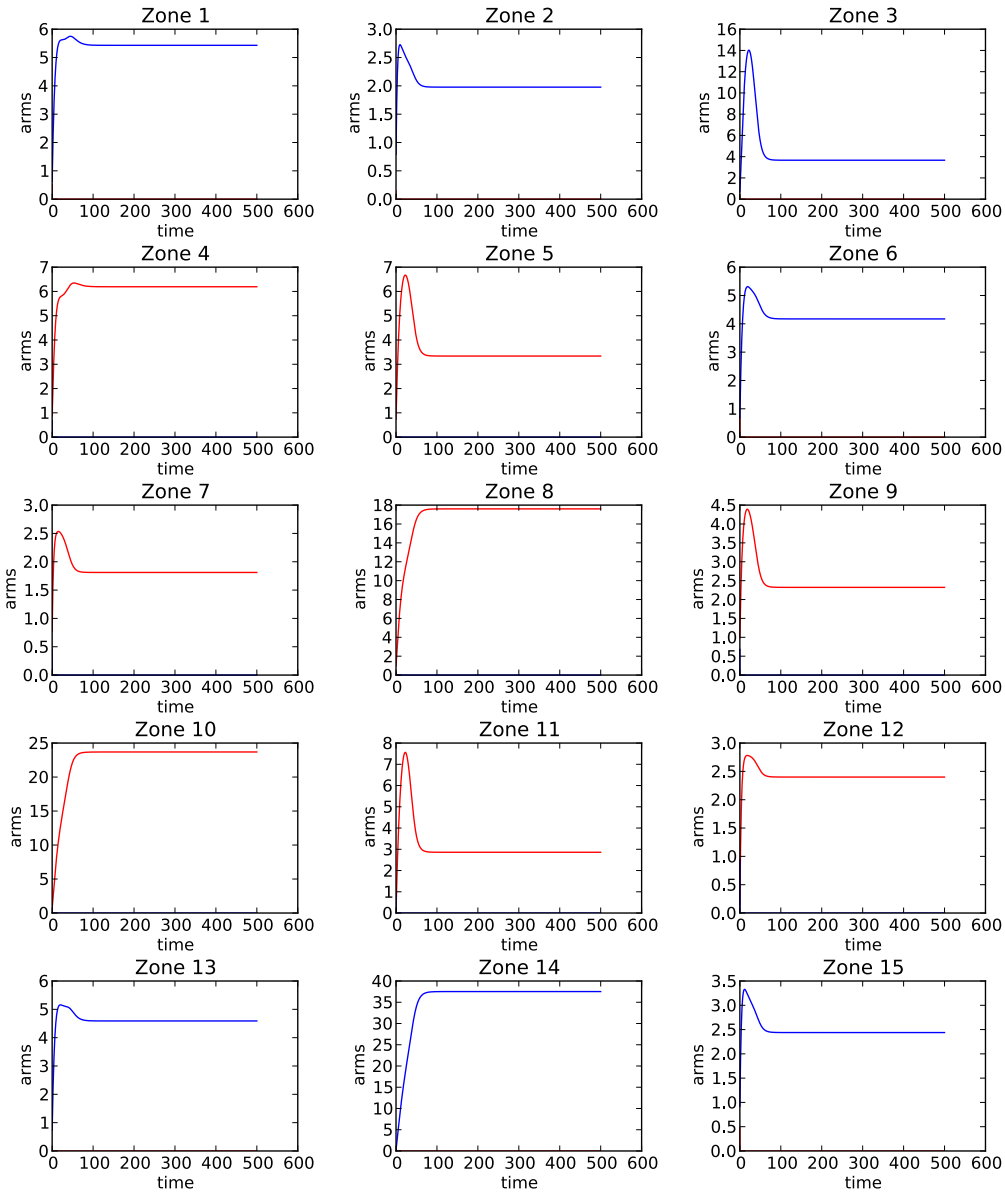

Figure 17: Results of the border dispute in each zone.

6 Discussion

We have developed a spatial extension to the Richardson model of conflict escalation. This is done by interpreting the coupling terms in the Richardson equations as the threat imposed by one team on the other and calculating the spatial distribution of this by using an entropy maximising spatial interaction model. This threat is then embedded within Richardson dynamics to model the escalation of conflict in space. By means of simulation, some features of this model have been analysed: effects of model parameters, including identification of various bifurcations; the effect of the spatial configuration of zones; and an idealised border dispute.

The main extension to this work will be to construct more realistic spatial models of both general and specific examples of combat and conflict. To achieve this, the Richardson dynamical model may not be sufficient. The spatial Richardson model, as described above, is used to investigate which spatial zones may experience escalation of conflict. For a more realistic model of combat, the following limitations come into play:

- there is no troop movement between the zones or overall conservation of resources;
- the cost of allocation of new arms is not included in the model;
- the fixed form of the dynamic element of the model does not allow for retreat or strategic aggression;
- 'grievance' and 'economic fatigue' would be difficult to determine in a data based simulation;
- Richardson dynamics may not be appropriate when the scenario has changed to one where changes in the variable of interest are caused by the decisions of an actor making strategic decisions.

Extensions planned at this stage involve addressing these limitations by considerating strategic allocation of a constrained number of resources; allowing resources, or military units, to move between zones - possibly at some cost; combat between adversaries in which military units are lost; replenishment of resources; consideration of supply chains (*e.g.* transporting weapons or sustenance to military units) and incorporating geographical information systems and infrastructure networks into the actions of the teams. Some of these may be achieved by spatially disaggregating the more general model, given in (1), or more specific dynamic ecological models that have been used for investigating conflict. Another route may be via a game-theoretical approach to explicitly consider the actions and strategies of actors involved in the conflict.

7 References

Epstein, J.M. (1997). Nonlinear dynamics, mathematical biology, and social science, Addison-Wesley Pub. Co.

Wilson, A. (2008). Boltzmann, Lotka and Volterra and spatial structural evolution: an integrated methodology for some dynamical systems. Journal of The Royal Society Interface, 5(25): 865-871.